Article
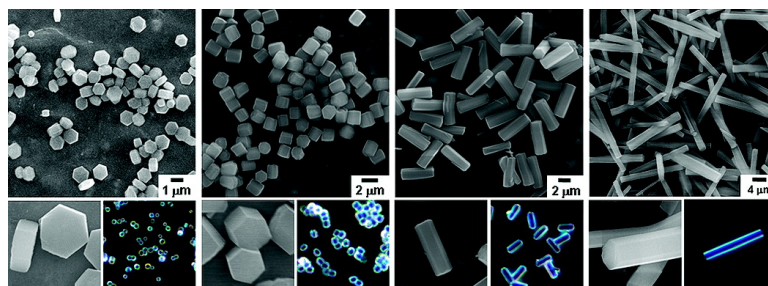
Growth-Controlled Formation of Porous Coordination Polymer Particles

Won Cho, Hee Jung Lee, and Moonhyun Oh

More About This Article

Additional resources and features associated with this article are available within the HTML version:

- Supporting Information
- Access to high resolution figures
- Links to articles and content related to this article
- Copyright permission to reproduce figures and/or text from this article

View the Full Text HTML

Growth-Controlled Formation of Porous Coordination Polymer Particles

Won Cho, Hee Jung Lee, and Moonhyun Oh*

Department of Chemistry, Yonsei University, 134 Shinchon-dong, Seodaemun-gu, Seoul 120-749, Korea

Received May 28, 2008; Revised Manuscript Received October 6, 2008; E-mail: moh@yonsei.ac.kr

Abstract: Diversely shaped porous coordination polymer particles (CPPs) were synthesized by a simple solvothermal reaction of 1,4-benzenedicarboxylic acid (H_2BDC) and $In(NO_3)_3 \cdot xH_2O$ in DMF. The growth of crystalline CPPs was controlled through a particle growth blocking event involving blocking agent interaction with particular facets of CPPs and simultaneous particle growth interruption in a specific direction. Systematic reactions in the presence of various amounts of pyridine as a blocking agent were conducted to see the controlled CPP formation. Long rod, short rod, lump, and disk-shaped CPPs with hexagonal faces resulted in the presence of none, 1 equiv, 2 equiv, and 25 equiv of pyridine, respectively. The ultimate particle shape produced depends upon the amount of blocking agents used.

Introduction

Porous coordination polymers have received a great deal of attention due to their useful applications in gas storage,[1−4] catalysis,[5] recognition,[6] and separation.[7] A structural study of macro-scaled crystalline samples was a main fundamental interest in coordination polymer materials. Recently, several groups have demonstrated a methodology to generate nano- and micro-scaled particles from infinite coordination polymers using several practical processes, such as precipitation,[8−12] solvothermal,[13,14] and reverse microemulsion[15] methods. For example, Mirkin's group[8,9] demonstrated the formation of chemically tailorable spherical coordination polymer particles (CPPs) by simply adding an initiation solvent to a precursor solution containing metal ions and metalloligands. Masel's group[14] prepared well-known metal-organic frameworks (MOFs)[16] as micro-sized cubic CPPs via a microwave-assisted solvothermal synthetic method. Lin et al.[15]
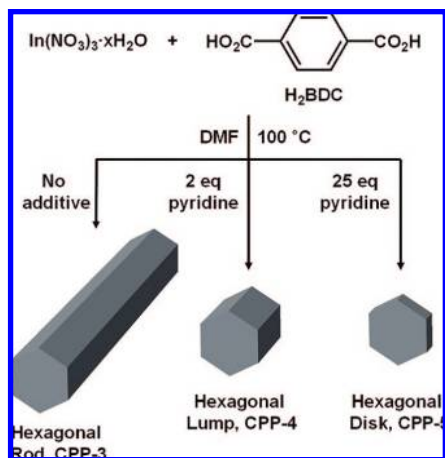
also reported the preparation of nanorod CPPs based on Gd(III) and BDC through general water-in-oil microemulsion-based methodology. Another class of materials, which are vital in optics,[17,18] catalysis,[19,20] medical diagnostics,[21] and biosensing,[22] are nano- and microparticles of metal, semiconductor, or metal alloy. Control over size and shape of particles is an important theme because this dictates the chemical and physical properties of particles.[23−28] Modulating growth rates of different crystal facets is a generally accepted and well-established method to finely control particle shape in preparing metal and semiconductor particles.[26−28]

A sophisticated understanding of coordination polymer particle formation, as well as the concomitant size and shape control, is crucial for the practical application of these materials. However, the fine control of CPP shape has not been well studied. In this paper, we describe a solvothermal approach to prepare porous CPPs from indium(III) and well-known 1,4-benzenedicarboxylate (BDC) building blocks. We also report

(1) Yaghi, O. M.; O'Keeffe, M.; Ockwig, N. W.; Chae, H. K.; Eddaoudi, M.; Kim, J. *Nature* **2003**, *423*, 705–714.
(2) Zhao, X.; Xiao, B.; Fletcher, A. J.; Thomas, K. M.; Bradshaw, D.; Rosseinsky, M. J. *Science* **2004**, *306*, 1012–1015.
(3) Maji, T. K.; Matsuda, R.; Kitagawa, S. *Nat. Mater.* **2007**, *6*, 142–148.
(4) Mulfort, K. L.; Hupp, J. T. *J. Am. Chem. Soc.* **2007**, *129*, 9604–9605.
(5) Seo, J. S.; Whang, D.; Lee, H.; Jun, S. I.; Oh, J.; Jeon, Y. J.; Kim, K. *Nature* **2000**, *404*, 982–986.
(6) Tabellion, F. M.; Seidel, S. R.; Arif, A. M.; Stang, P. J. *J. Am. Chem. Soc.* **2001**, *123*, 7740–7741.
(7) Kosal, M. E.; Chou, J.-H.; Wilson, S. R.; Suslick, K. S. *Nat. Mater.* **2002**, *1*, 118–121.
(8) Oh, M.; Mirkin, C. A. *Nature* **2005**, *438*, 651–654.
(9) Oh, M.; Mirkin, C. A. *Angew. Chem., Int. Ed.* **2006**, *45*, 5492–5494.
(10) Sun, X.; Dong, S.; Wang, E. *J. Am. Chem. Soc.* **2005**, *127*, 13102–13103.
(11) Park, K. H.; Jang, K.; Son, S. U.; Sweigart, D. A. *J. Am. Chem. Soc.* **2006**, *128*, 8740–8741.
(12) Wei, H.; Li, B.; Du, Y.; Dong, S.; Wang, E. *Chem. Mater.* **2007**, *19*, 2987–2993.
(13) Jung, S.; Oh, M. *Angew. Chem., Int. Ed.* **2008**, *47*, 2049–2051.
(14) Ni, Z.; Masel, R. I. *J. Am. Chem. Soc.* **2006**, *128*, 12394–12395.
(15) Rieter, W. J.; Taylor, K. M. L.; An, H.; Lin, W.; Lin, W. *J. Am. Chem. Soc.* **2006**, *128*, 9024–9025.

(16) Eddaoudi, M.; Kim, J.; Rosi, N.; Vodak, D.; Wachter, J.; O'Keeffe, M.; Yaghi, O. M. *Science* **2002**, *295*, 469–472.
(17) Wang, J.; Gudiksen, M. S.; Duan, X.; Cui, Y.; Lieber, C. M. *Science* **2001**, *293*, 1455–1457.
(18) Fleischhaker, F.; Arsenault, A. C.; Kitaev, V.; Peiris, F. C.; von Freymann, G.; Manners, I.; Zentel, R.; Ozin, G. A. *J. Am. Chem. Soc.* **2005**, *127*, 9318–9319.
(19) Bell, A. T. *Science* **2003**, *299*, 1688–1691.
(20) Kim, S.-W.; Kim, M.; Lee, W. Y.; Hyeon, T. *J. Am. Chem. Soc.* **2002**, *124*, 7642–7643.
(21) Gao, X.; Cui, Y.; Levenson, R. M.; Chung, L. W. K.; Nie, S. *Nat. Biotechnol.* **2004**, *22*, 969–976.
(22) Cao, Y. C.; Jin, R.; Mirkin, C. A. *Science* **2002**, *297*, 1536–1540.
(23) Sun, S.; Murray, C. B.; Weller, D.; Folks, L.; Moser, A. *Science* **2000**, *287*, 1989–1992.
(24) Horn, D.; Rieger, J. *Angew. Chem., Int. Ed.* **2001**, *40*, 4330–4361.
(25) Chen, J.; Herricks, T.; Xia, Y. *Angew. Chem., Int. Ed.* **2005**, *44*, 2589–2592.
(26) Mokari, T.; Zhang, M.; Yang, P. *J. Am. Chem. Soc.* **2007**, *129*, 9864–9865.
(27) Peng, X.; Manna, L.; Yang, W.; Wickham, J.; Scher, E.; Kadavanich, A.; Alivisatos, A. P. *Nature* **2000**, *404*, 59–61.
(28) Manna, L.; Milliron, D. J.; Meisel, A.; Scher, E. C.; Alivisatos, A. P. *Nat. Mater.* **2003**, *2*, 382–385.

useful methodology to control CPP shape through modulating the growth rate of different facets of crystalline CPP. As described in Scheme 1, CPPs were selectively generated with hexagonal rod (CPP-3), hexagonal lump (CPP-4), and hexagonal disk shapes (CPP-5).

Results and Discussion

Micro-sized rods with a hexagonal face (CPP-3) were synthesized by the following straightforward process: 1,4-benzenedicarboxylic acid (H_2BDC) was dissolved in *N,N*-dimethylformamide (DMF), and DMF containing $In(NO_3)_3 \cdot xH_2O$ was added to the prepared solution. The resulting mixture was heated at 100 °C for 10 min (Scheme 1). The product generated in this time was isolated by cooling the reaction mixture to room temperature, collecting the precipitate by centrifugation, and washing several times with DMF and methanol.

Field-emission scanning electron microscopy (SEM) and optical microscopy (OM) images of CPP-3 (Figure 1) reveal hexagonal rod formation with an average width of 1.75 ± 0.24 μm and length of 16.3 ± 1.6 μm. The chemical composition of CPP-3 was determined by energy dispersive X-ray (EDX, Figure 2a) spectroscopy, elemental analysis (EA) (see Experimental Section), and ^{1}H NMR spectroscopy (see Supporting Information). Even though hexagonal rod CPP-3 is stable in several organic solvents, including DMSO and DMF, it can be digested into individual building blocks by adding organic acids. Therefore, one can determine the amount of building blocks
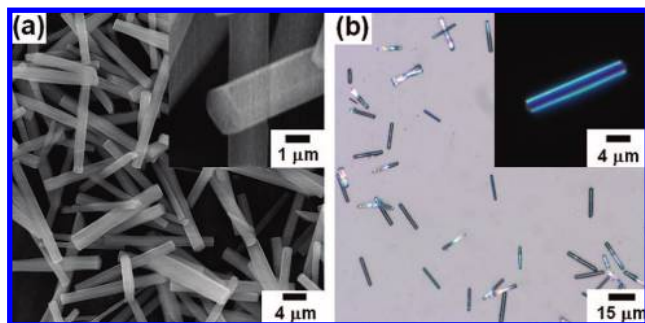
Figure 1. (a) SEM images (inset is high-magnification image) and (b) bright-field OM image (inset is high-magnification dark-field image) of hexagonal rods (CPP-3) with an average width and length of 1.75 ± 0.24 and 16.3 ± 1.6 μm, respectively (SD, $n = 100$).
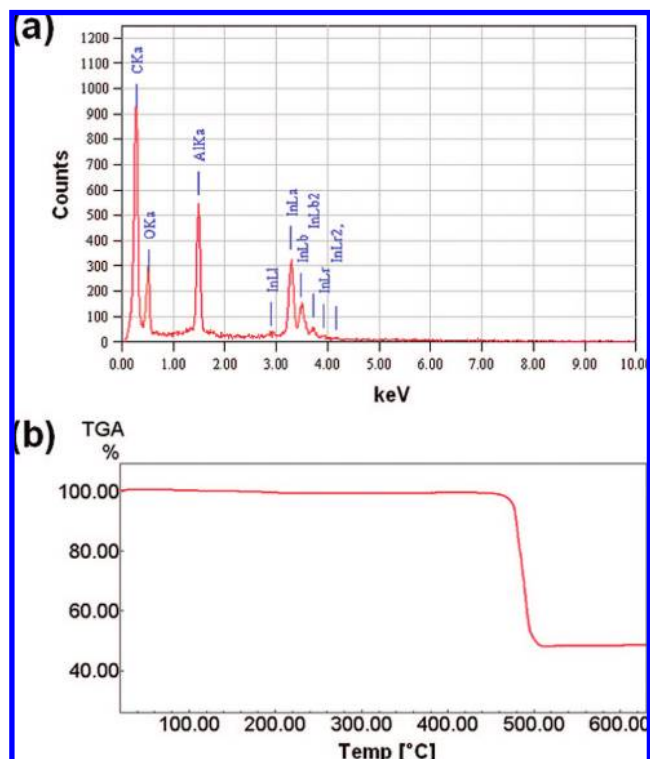
Figure 2. (a) EDX spectrum and (b) TGA curve of hexagonal rods (CPP-3).

incorporated within CPP-3. The incorporation of one BDC molecule per In^{3+} in CPP-3, obtained from the ^{1}H NMR spectrum of CPP-3 digested in acetic acid-d_4 and DMSO-d_6, is consistent with EA result. In coordination chemistry, the creation of coordination polymers can be expediently characterized by infrared (IR) spectroscopy.[1−16] The IR spectrum of CPP-3 confirms the coordination of the carboxylate groups of BDC to In^{3+} ions, as evidenced by a shift in the CO stretching frequency to 1558.2 $cm^{−1}$. This value can be compared to the CO stretching frequency of 1685.9 $cm^{−1}$ for the unco-ordinated H_2BDC. The resulting CPP-3 was found to be thermally stable to 460 °C, by thermogravimetric analysis (TGA, Figure 2b). Furthermore, TGA data reveal that no significant guest molecules are involved in CPP-3 after conventional vacuum treatment, as evidenced by no substantial weight loss until 460 °C.

CPP-3 is considered to be a permanently porous material based on the TGA and gas sorption measurements. All gas sorption isotherms were measured after pretreatment under a dynamic vacuum at 250 °C. As shown in Figure 3a, the N_2 sorption isotherm shows type I behavior typical for microporous materials.[29] The BET and Langmuir surface areas of CPP-3 obtained from the adsorption branch of the isotherm are 1730.6 and 1860.2 m^2/g, respectively. The isotherm is totally reversible, and the total pore volume is 0.6101 cm^3/g. The hydrogen storage capacity of CPP-3 at 77 K and under <1 atm is shown in Figure 3b. The isotherm is reversible, and hydrogen uptake is 1.25 wt % (volumetric uptake of 140.00 cm^3/g). Furthermore, the CO_2 uptake of CPP-3 was measured at 195 K (Figure 3c); the isotherm is reversible again and the maximum uptake is 333.45 cm^3/g.

Using the surfactant effect to control the growth direction of metallic or semiconducting crystalline nanomaterials is well

(29) IUPAC., *Pure Appl. Chem.* **1985**, *57*, 603–619.
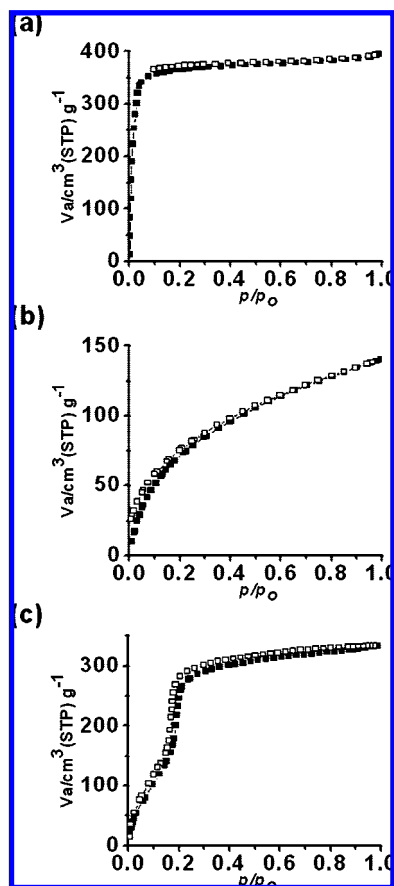
Figure 3. Adsorption−desorption isotherms of CPP-3 for (a) N_2 adsorption (solid symbol) and desorption (open symbol) at 77 K, (b) H_2 adsorption (solid symbol) and desorption (open symbol) at 77 K, and (c) CO_2 adsorption (solid symbol) and desorption (open symbol) at 195 K.
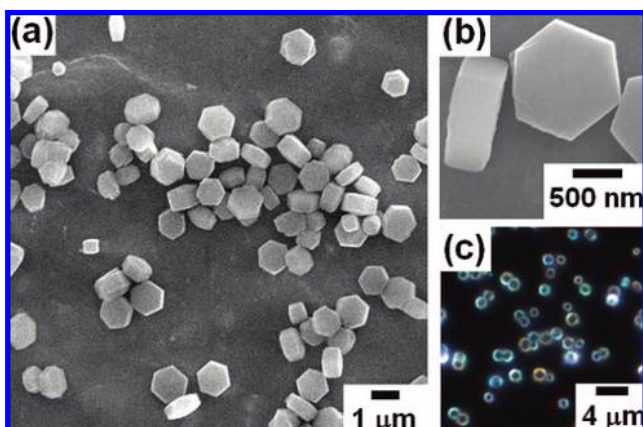
Figure 4. (a) Low-magnification SEM image, (b) high-magnification SEM image, and (c) dark-field OM image of hexagonal disks (CPP-5) with an average width and length of 970 ± 94 and 429 ± 64 nm, respectively (SD, n = 100).

studied and generally used to control shape.[26−28] We have investigated this method to control CPP growth. Interestingly, SEM images of CPPs obtained in the presence of excess pyridine under otherwise identical conditions as described above show the formation of hexagonal disk structures (CPP-5) instead of hexagonal rods. As shown in SEM and OM images in Figure 4, the morphology of CPP-5 is a hexagonal disk with an average width and thickness of 970 ± 94 and 429 ± 64 nm, respectively. The formation of hexagonal disks instead of hexagonal rods
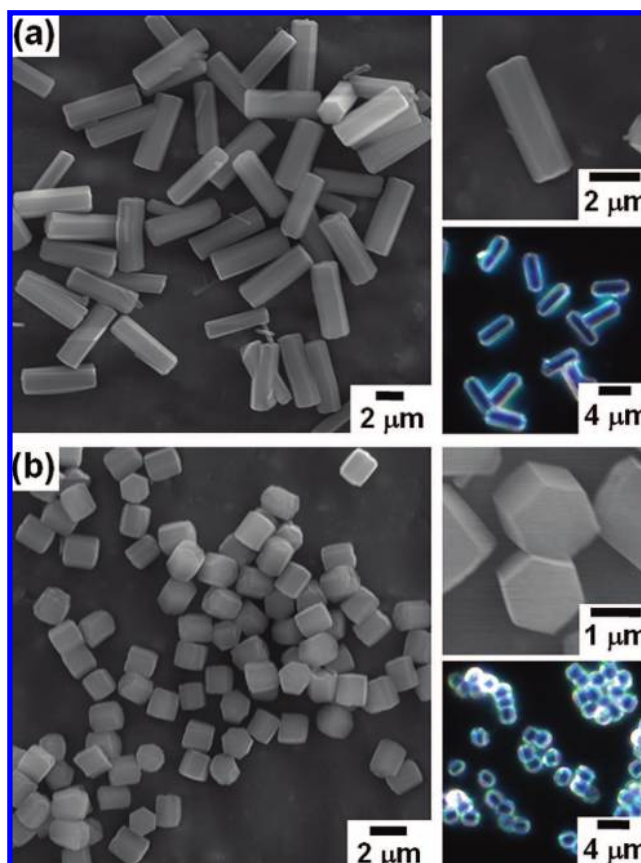
Figure 5. SEM (left and top right) and dark-field OM (bottom right) images of (a) hexagonal rods (CPP-3′) with an average width and length of 1.64 ± 0.20 and 4.81 ± 0.28 μm, respectively (SD, n = 100), and (b) hexagonal lumps (CPP-4) with an average width and length of 1.59 ± 0.14 and 1.75 ± 0.19 μm, respectively (SD, n = 100).

can be rationalized by a blocking event in which pyridine reversibly coordinates to an indium center exposed on the hexagonal facet of CPPs[27,28,30] and simultaneously blocks particle growth in that direction. Powder X-ray diffraction (PXRD) spectra of CPP-3 and CPP-5 reveal that both particles have the same structure (see Supporting Information). In addition to PXRD spectra, all IR and EDX spectra, EA data, and gas sorption measurements of CPP-3 and CPP-5 confirm that they are the same materials with identical inner structures but different outer shapes (see Experimental Section and Supporting Information).

We have carried out systematic reactions in the presence of various amounts of pyridine as a blocking agent to see the controlled CPP growth. In the presence of a small amount of pyridine (1 equiv), hexagonal rods (CPP-3′) with an average width and length of 1.64 ± 0.20 and 4.81 ± 0.28 μm, respectively, were generated (Figure 5a). By increasing the amount of pyridine to 2 equiv, the particle length was reduced to 1.75 ± 0.19 μm while maintaining the hexagonal feature (Figure 5b). This product is more likely a hexagonal lump (CPP-4) than a hexagonal rod. In both CPP-3′ and CPP-4, the lengths of the resulting particles are dramatically reduced to 4.81 and

(30) There are inherent difficulties in finding the exact structure of nano- and micro-scaled CPPs; the hexagonal facet of CPPs may have a different nature from the lateral facet, as shown in the single-crystal X-ray structure of [In(OH)(BDC)]$_n$. Anokhina, E. V.; Vougo-Zanda, M.; Wang, X.; Jacobson, A. J. *J. Am. Chem. Soc.* **2005**, *127*, 15000–15001.

1.75 μm, respectively, compared to 16.3 μm for CPP-3 generated in the absence of pyridine. However, the widths of the resulting particles are almost the same regardless of pyridine (1.75 μm for CPP-3, 1.64 μm for CPP-3′, 1.59 μm for CPP-4). All PXRD, IR, and EDX spectra, EA data, and gas sorption measurement on N_2 of CPP-4 reveal that it has an identical inner structure to CPP-3 and CPP-5. From this series of experiments, we can conclude that the blocking efficiency during particle growth can be controlled by the amount of blocking agent used. In the presence of excess pyridine, particle growth in the direction of the hexagonal facet is effectively blocked, resulting in hexagonal disks. In the presence of a small amount of pyridine, however, the blocking agents inefficiently delay the CPP growth, resulting in hexagonal lumps and short hexagonal rods. In the absence of pyridine, hexagonal rods were formed due to no growth delay. In addition, the acceleration of the deprotonation of H_2BDC in the presence of pyridine cannot be ruled out in the formation of CPPs. By utilizing this methodology, one can systematically control CPP length and thus CPP shape.

Conclusions

In summary, this article demonstrates that modulating the growth rates of crystalline coordination polymer particles (CPPs) can be used to control CPP shape, through a particle growth blocking event involving the interaction of blocking agents with particular facets of CPPs and the simultaneous particle growth interruption in a specific direction. In this manner, the particle growth rate in certain direction can be manipulated by the amount of blocking agent used. Thus different CPP shapes such as hexagonal rods, hexagonal lumps, and hexagonal disks selectively resulted. The growth control and shape change demonstrated in this paper should be of core assistance in developing CPP materials and in rational control of CPP properties.

Experimental Section

Solvents and all other chemicals were obtained from commercial sources and used as received unless otherwise noted. Infrared spectra of solid samples were obtained on a Nicolet Avatar 360 FT-IR spectrometer as KBr pellet. Elemental analyses were performed at Organic Chemistry Reaction Center, Sogang University. All scanning electron microscopy (SEM) images and energy dispersive X-ray (EDX) spectra were obtained using a Hitachi S-4300 field-emission SEM equipped with a Horiba EMAX 6853-H EDS system (Center for Microcrystal Assembly, Sogang University) or JEOL JSM-6500F field-emission SEM equipped with a JEOL EX-23000 BU EDS system (Yonsei Nanomedical National Core Research Center). All bright-field and dark-field optical microscopy images were obtained using a Zeiss Axio Observer. D1m optical microscope equipped with a AxioCam MRc 5 digital camera. ^1H NMR spectra were recorded on a Bruker Advance/DPX 250 (250 MHz ^1H) spectrometer with chemical shifts reported relative to residual

deuterated solvent peaks. X-ray diffraction studies were conducted using a Rigaku D/MAX-RB equipped with a graphite-monochromated Cu Kα radiation source (40 kV, 120 mA). TGA was carried out with a Shimadzu TGA-50 in a nitrogen atmosphere. All TGA were measured after pretreatment under a dynamic vacuum at room temperature. Adsorption−desorption isotherms for CO_2 (195 K), N_2 (77 K), and H_2 (77 K) were measured in the gaseous state by using BELSORP II-mini volumetric adsorption equipment. All gas sorption isotherms were measured after pretreatment under a dynamic vacuum at 250 °C.

Preparation of Hexagonal Rods CPP-3. A precursor solution was prepared by mixing 1,4-benzenedicarboxylic acid (H_2BDC, 3.0 mg) and $In(NO_3)_3 \cdot xH_2O$ (7.8 mg) in 0.9 mL of DMF. The resulting mixture was placed in an oil bath (100 °C) for 10 min. Hexagonal rods (CPP-3) generated in this time were isolated by cooling the reaction mixture to room temperature, collecting the precipitate by centrifugation, and washing several times with DMF and methanol. Each successive supernatant was decanted and replaced with fresh DMF and methanol (32−85% yield). The yield depends upon the amount of solvent used. When a small amount of solvent is used, the large hexagonal rods were obtained with a high yield. IR (KBr pellet, cm^{-1}): 1558.2s, 1505.7m, 1397.4s, 1316.3w, 1175.5w, 1153.7w, 1106.5w, 1018.6m, 881.0m, 823.2w, 812.6w, 747.9m, 551.2m. Anal. Calcd for CPP-3 $[In(OH)(BDC)]_n$: C, 32.47; H, 1.70. Found: C, 32.41; H, 1.71. The formula of CPP-3 was suggested by the ^1H NMR spectrum of CPP-3 digested in acetic acid-d_4 and DMSO-d_6, EA data, and the related compound.[30] The ^1H NMR spectrum of the digested particles shows one BDC molecule per In^{3+} in CPP-3.

Preparation of Hexagonal Lumps CPP-4. CPP-4 was prepared in the presence of 2 equiv of pyridine under otherwise identical reaction conditions to those described above (57% yield). IR (KBr pellet, cm^{-1}): 1558.3s, 1505.3m, 1395.8s, 1316.8w, 1175.5w, 1154.0w, 1105.5w, 1018.9m, 881.9m, 823.2w, 813.1w, 748.4m, 550.4m. Anal. Calcd for CPP-4 $[In(OH)(BDC)]_n$: C, 32.47; H, 1.70. Found: C, 32.44; H, 1.76.

Preparation of Hexagonal Disks CPP-5. CPP-5 was prepared in the presence of 25 equiv of pyridine under otherwise identical reaction conditions to those described above (62% yield). IR (KBr pellet, cm^{-1}): 1558.6s, 1505.4m, 1394.5s, 1316.5w, 1171.9w, 1157.2w, 1103.4w, 1019.6m, 881.6m, 823.2w, 812.8w, 748.1m, 551.0m. Anal. Calcd for CPP-5 $[In(OH)(BDC)]_n$: C, 32.47; H, 1.70. Found: C, 32.50; H, 1.79.

Supporting Information Available: PXRD, NMR spectra, and adsorption−desorption isotherm data. This material is available free of charge via the Internet at http://pubs.acs.org.

JA8039794